Hindawi Publishing Corporation
EURASIP Journal on Advances in Signal Processing
Volume 2009, Article ID 238103, 16 pages
doi:10.1155/2009/238103

Research Article

Enhancing the Performance of Random Access Networks with Random Packet CDMA and Joint Detection

Roland Kempter,[1] Peiman Amini,[2] and Behrouz Farhang-Boroujeny[2]

[1] *Military Air Systems, EADS Deutschland GmbH, 88039 Friedrichshafen, Germany*
[2] *Department of Electrical and Computer Engineering, University of Utah, UT 84112, USA*

Correspondence should be addressed to Roland Kempter, kempter@ece.utah.edu

Received 17 January 2008; Revised 17 April 2008; Accepted 29 July 2008

Recommended by Petar Popovski

Random packet CDMA (RP-CDMA) is a recently proposed random transmission scheme which has been designed from the beginning as a cross-layer method to overcome the restrictive nature of the Aloha protocol. Herein, we more precisely model its performance and investigate throughput and network stability. In contrast to previous works, we adopt the spread Aloha model for header transmission, and the performance of different joint detection methods for the payload data is investigated. Furthermore, we introduce performance measures for multiple access systems based on the diagonal elements of a modified multipacket reception matrix, and show that our measures describe the upper limit of the vector of stable arrival rates for a finite number of users. Finally, we simulate queue sizes and throughput characteristics of RP-CDMA with various receiver structures and compare them to spread Aloha.

1. Introduction

Generally, channel access can be performed either in a centrally controlled or distributed fashion. The benefit of scheduled access is obvious: due to the all-knowing nature of the channel arbiter (i.e., the base station), packet collisions can be avoided and service can be guaranteed [1]. However, these benefits come at the price of signaling overhead [2]. Additionally, in ad hoc networks, scheduled access is mostly avoided because of signaling complexity and/or signaling overhead. As a result, distributed, "handshake-free" random channel access has not only attracted considerable attention in data networks, but has in fact conquered this scenario. As an example, in packetized data networks where channel sensing is possible, the IEEE 802.11 standard has sparked a breakthrough of wireless technology. Where sensing is not feasible, random access is typically facilitated through the Aloha protocol or one of its flavors [3, 4]. Such environments include networks with large propagation delay, for instance, satellite communication systems. Unfortunately, the lack of sensing greatly reduces the achievable throughput and the rate region where network stability can be guaranteed [4, 5].

Random packet code division multiple access (RP-CDMA) [6] is a recently proposed random transmission scheme which has been designed to ease the performance penalties associated with fully random network operation. RP-CDMA embodies a cross-layer design approach for the physical and MAC layers to overcome the restrictive nature of the Aloha method. As has been shown in [6], RP-CDMA has the potential to greatly improve system throughput and to approach the goodput ("raw" channel capacity minus signaling overhead) of scheduled channel access. This is achieved through a reduction of the probability of packet collisions combined with multiuser detection technology to resolve multiuser interference. Essentially, the RP-CDMA physical layer allows for multipacket reception, hence, multiuser receivers are able to improve its throughput. At the same time, RP-CDMA maintains the simple MAC layer of the original Aloha protocol without the need for channel sensing. Furthermore, the performance of RP-CDMA can improve with the capabilities of the base station, no modifications in the transmitters are necessary.

In RP-CDMA, a transmitted packet of length $(L_h + L_d)$ consists of header and data portions as illustrated in Figure 1.

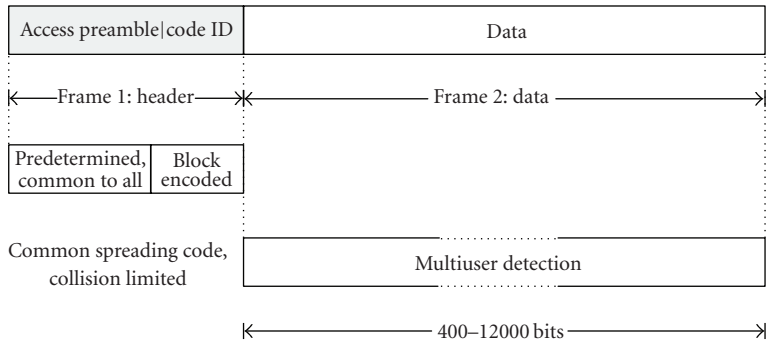

Figure 1: RP-CDMA packet format as proposed in [6].

The header frame of length L_h consists of the access preamble necessary for packet detection and carrier as well as timing recovery. The headers are all spread with a unique spreading signature which is known universally and contain the randomly chosen spreading information (Code ID) used to encode the data portion of the packet. For the data portion, the probability that any two active frames employ identical spreading sequences which would lead to collisions can be made arbitrarily small by increasing the Code ID. The header sequence enables the base station to detect ongoing concurrent transmissions and to recover timing information for each packet, allowing RP-CDMA to be fully asynchronous. Essentially, the header channel operates a spread Aloha system under extremely low load, thus facing a very low probability of packet collisions, whereas data transmission occurs under 3G CDMA system-like conditions.

In [6], the system characteristics of RP-CDMA have been investigated under the assumption of a collision-limited Aloha header process, setting the effects of multiuser interference aside. In addition, no method for the detection of the data frame of the packet was introduced or discussed. Instead, it was assumed that as long as the headers survive, successful recovery of the entire packet is guaranteed using *ideal* multipacket capture technology. Also, sizes of the data frame of the RP-CDMA packet in the order of hundreds of thousands of bytes were required to improve system throughput. As a result of these specific assumptions, it was concluded that RP-CDMA allows to approach the capacity of the multiaccess channel, and system performance is only limited by the capabilities of the base station in terms of the number of decodeable concurrent transmissions.

Herein, a more complete and realistic analysis of RP-CDMA is presented. In essence, we take into account realistic physical layer limitations, which allows us to understand RP-CDMA's properties in an integrated fashion—across the boundaries formed by it's physical and MAC layers. In a sense, the RP-CDMA packet format separates the wireless channel into two virtual channels: one for header and one for data transmission. We study the performance of both virtual channels for more general sizes of the data frame. Earlier analysis is extended in the following ways.

(1) Header transmission faces two limitations: (i) a collision limitation on the chip-level due to identical header spreading sequences, and (ii) an interference limitation caused by concurrent headers and, especially, data transmissions. We consider both of these effects in our analysis.

(2) We investigate the behavior of the matched filter, the MMSE, the decorrelation receiver, as well as partitioned spreading demodulation for the data frame of the RP-CDMA packet in a multipacket capture channel.

(3) As has been shown and derived analytically by Naware, Mergen, and Tong in [5, 7, 8], we are able to base our performance analysis on the diagonal elements of the modified multipacket reception matrix $\widetilde{\mathbf{E}}$; namely, Λ_n and $\sum_n \Lambda_n = \zeta$. It also follows from those references that Λ_n serves as the upper limit of the stable arrival rates for n users. Using those metrics, we present more detailed and realistic results for the possibilities as well as limitations of RP-CDMA header and data transmission than those derived in [6].

(4) The system is simulated for different receiver structures and performance in terms of queue size, and throughput is investigated.

Our paper is organized as follows. In Section 2, we introduce some notation and discuss preliminary assumptions, followed by an introduction to the multipacket reception channel and our performance metrics in Section 3. We proceed with an evaluation of the performance of spread Aloha and the RP-CDMA header process under various limiting assumptions in Section 4. In Section 5, we present the capabilities of RP-CDMA data recovery with our different receiver technologies. Section 6 combines "all the pieces" via network-level simulations of RP-CDMA. Finally, Section 7 concludes our paper.

2. Notation and Preliminaries

2.1. Notation. We denote the processing gain by N with subscripts d indicating the RP-CDMA data and h indicating the RP-CDMA header frames; similarly, N_{SA} indicates

the spreading gain of spread Aloha. The lengths of the RP-CDMA header and payload frames are denoted as L_h and L_d, respectively. Γ is used to denote the signal-to-interference-plus-noise ratio (SINR) at the output of a receiver, and γ refers to the detection threshold. K denotes the overall network population, out of which n users are active at a given time. We assume fixed bit durations; accordingly, when the processing gain N is increased, the chip size reduces proportional to $1/N$, and the required bandwidth increases proportional to N. As a result, any increase of N constitutes a loss of bandwidth efficiency.

2.2. CDMA System Model. We assume $n \in K$ active users with independently generated binary information bits $b_k(i) \in \{0, 1\}$, $k = 1, \ldots, n$ and modulated by n signature sequences $\{s_k(t)\}_{k=1}^{n}$. As is common in the literature and for mathematical purposes only, (see, e.g., [9–12]), we assume chip syncronicity. The transmitted signals are embedded in an additive white Gaussian noise (AWGN) channel and the received CDMA signal is

$$y(t) = \sum_{k=1}^{n} \sqrt{E_k} x_k(t) + \nu(t), \tag{1}$$

where E_k is the power of the kth user, $\nu(t)$ is zero-mean white Gaussian noise with two-sided spectral density σ^2, $x_k(t) = \sum_i b_k(i) s_k(t - iT)$, and T is the bit interval. The chip synchronicity assumption can be removed through a more cumbersome analysis which on average leads to similar results (see [13]).

2.3. Analytical Analysis: Asynchronous Versus Synchronous Packet Transmission. For analytical analysis of RP-CDMA, we assume packet level synchronicity, that is, packets are transmitted in predefined time slots. At a first glance, this seems like a violation of its envisioned asynchronous mode of operation. However, as far as the level of interference at the receiver, caused by asynchronous versus synchronous arrivals, is concerned, we note that the signal-to-noise ratio has to be interpreted as an average over the *entirety of all* received packets. Along these lines, the performance of large powerful error control codes, such as turbo or LDPC codes [14]—which we envision to be used for payload encoding in any wireless transmission scheme—essentially follows the average SINR over the frame. Hence, only a small error is made by applying a synchronous model to the originally fully asynchronous RP-CDMA system.

While the assumption of packet level synchronicity allows us to grasp the characteristics of the interference process at the receiver, it would automatically lead to header collisions due to chip-level synchronicity. However, we can resolve this issue if we allow the starting point of our headers to be randomly distributed throughout the overall length of the RP-CDMA packet. We want to point out, thanks to these manipulations only, that we are able to come to a better mathematical understanding of the properties of RP-CDMA network operation. To our best knowledge, only few steps have been made towards true asynchronous analytical network analysis, and the usability of the derived mathematical models seems very limited and highly restrictive (see, e.g., [15]).

Of course, we only use these assumptions for our analytical analysis. Whenever we present simulations results, RP-CDMA operates as described in Section 1, and we want to point out the very good match between the two.

2.4. Traffic Model. For our investigations, we adopt a widely used model for the classification of the physical layer performance of Aloha-type multiaccess systems. In accordance with [3–5, 7, 16–24], we assume that packets are generated independently according to a Bernoulli process with rate λ, $0 \leq \lambda \leq 1$, and each node has a queue for storing the generated packets. From the queues, the first packet in the queue is transmitted with probability $P = 1$ in the next time slot. If a packet has not been received correctly, in addition to any newly generated packets, it reenters the queue and is retransmitted in the subsequent time slot and feedback is instantaneous and error-free. $P = 1$ is chosen based on the discussion on the optimality of *persistent Aloha* in the case of multipacket capture in [5]. Also from a systems angle, we believe it is very reasonable for an RP-CDMA implementation to immediately transmit packets as they enter the nodes' queues as an approach to reduce transmission delay—comparable to *1-persistent CSMA/CD* (see, e.g., [25]). Also note that $P = 1$ is the underlying assumption in the definition of the multipacket capture matrix $\mathbf{E}$, [22], which is defined below.

3. Multiuser Systems and Performance Metrics

3.1. Definitions. Given that n packets are being transmitted in a slot, for $n \geq 1$, $0 \leq k \leq n$, we define

$$\epsilon_{n,k} \Pr(k \text{ packets are received correctly} \mid n \text{ are transmitted}). \tag{2}$$

The multipacket reception property of a receiver can be described by the multipacket reception matrix, $\mathbf{E}$ [22]:

$$\mathbf{E} = \begin{pmatrix} \epsilon_{1,0} & \epsilon_{1,1} & 0 & \cdots & 0 \\ \epsilon_{2,0} & \epsilon_{2,1} & \epsilon_{2,2} & \ddots & \vdots \\ \vdots & \vdots & \vdots & \ddots & 0 \\ \epsilon_{n,0} & \epsilon_{n,1} & \epsilon_{n,2} & \cdots & \epsilon_{n,n} \end{pmatrix}. \tag{3}$$

Accordingly, system throughput when m packets are being transmitted is computed as

$$S_m = \sum_{k=1}^{m} k \epsilon_{m,k}. \tag{4}$$

Along these lines, it is obvious that the optimal multiaccess system is the one that is able to guarantee successful detection for all active transmissions.

We also define the modified $n \times n$ multipacket reception matrix $\widetilde{\mathbf{E}}$, which is obtained from $\mathbf{E}$ by removing its first column, that is,

$$\widetilde{\mathbf{E}} = \begin{pmatrix} \epsilon_{1,1} & 0 & \cdots & 0 \\ \epsilon_{2,1} & \epsilon_{2,2} & \ddots & \vdots \\ \vdots & \vdots & \ddots & 0 \\ \epsilon_{n,1} & \epsilon_{n,2} & \cdots & \epsilon_{n,n} \end{pmatrix}. \tag{5}$$

In this paper, we follow Loynes [26] and refer to a system as stable when the queue sizes in the nodes converge to a finite number as time goes to infinity.

3.2. Performance Metrics for Multiaccess Systems: $\mathbf{\Lambda}$ and ζ. In the remainder, we calculate, simulate, and compare network performance under various conditions and detectors. Here, we present measures that we found suitable for our study. In the literature, typically system throughput S as a function of the load G is used for comparisons. However, it is a well-observed fact that in random schemes, obtaining maximum throughput with a finite number of users comes at the price of infinite queue sizes, that is, network instability (see, e.g., [1, 3, 26–28]). Hence, throughput alone is *not* a meaningful measure for the performance of multiaccess systems, and researchers have used delay in addition to throughput. However, this makes the prediction of network performance hard if not unfeasible, since the quality of an accessing technique is not easily captured analytically. In fact, network-level performance limits are typically found through simulation, while only in some special cases in the *collision channel*, analytical models are available (see, e.g., [25, 29, 30]). What makes matters more complicated in the case of RP-CDMA and spread Aloha is the fact that in the multiuser channel, multiple simultaneous transmissions not only may be successful but are in fact a feature to reduce delay and increase throughput. In fact, one may understand such multiuser systems as a set of (pseudo-) parallel channels that are correlated to some degree as a function of various receiver and network parameters. Considerable effort has gone into analytically predicting the stable-rate regions for the general case of $n > 3$ users—albeit without much success (see [5, 19] for a discussion). Based on $\widetilde{\mathbf{E}}$, we show that at least in an environment with power control (all nodes are received at the same power level), the properties of the multipacket capture matrix itself allow us to express the maximum stable *arrival rates* (λ_n) given some $\widetilde{\mathbf{E}}$. The reason is as follows: the vector of the diagonal elements of $\widetilde{\mathbf{E}}^{(\mathrm{opt})}$ of an optimal multiaccess system with K users has exactly K elements of value 1:

$$\mathrm{diag}\left(\widetilde{\mathbf{E}}^{(\mathrm{opt})}\right) = \mathbf{1}, \tag{6}$$

where $\mathbf{1}$ is a $1 \times K$ vector, that is, $\widetilde{\mathbf{E}} = \mathbf{I}$.

Hence,

$$\zeta = \sum \mathrm{diag}\left(\widetilde{\mathbf{E}}^{(\mathrm{opt})}\right) = K, \tag{7}$$

and we denote the vector of the diagonal elements of $\widetilde{\mathbf{E}}$ as $\mathbf{\Lambda}$.

Note that $\mathbf{\Lambda}$ represents the transmissions for which $k = n$, that is, all the transmitted packets which are received correctly. As stated previously, the number of nonzero elements on the diagonal of $\widetilde{\mathbf{E}}$is the number of parallel channels provided by the system—correlated if $\epsilon_{n,k} < 1$. To elaborate, based on the results presented in [5, 7, 8], we can calculate the elements on the diagonal of $\widetilde{\mathbf{E}}$ and use them as a measure of the number of parallel channels and the degree of their independence obtained through a specific method of multipacket reception. Furthermore, in a base station centric system, there is exactly one server for n customers. From the necessary condition for queue stability, which requires that the average arrival rate λ needs to be smaller than the average service rate $\mathbf{\Lambda}$, multiplied by the number of servers in the system, we are left with the trivial finding that Λ_n directly represents the upper limit on the stable arrival rates λ_n for a number of $1 \leq n \leq K$ homogeneous (equal arrival rate, equal power) users. We support this idea through simulations in Section 6.

Also, the closer ζ is to K, the more parallel "channels" are provided and hence ζ is a measure of the optimality of a multiaccess system. This means that the elements of $\mathbf{\Lambda}$ are a measure for the degree of orthogonality between the transmissions, and they can thus be used to determine the maximum arrival rates on these channels. As a result, we define $\eta = \zeta/K \leq 1$ as our quality of service (QoS) parameter.

4. The Performance of RP-CDMA Header Detection and Similarities to Spread Aloha

The successful reception of a user's packet in RP-CDMA requires correct header as well as correct data detection. We examine these factors individually, noting that packet transmission can be separated into two virtual channels—a header and a data channel (see Figure 2). For one, header reception is affected by packet collisions on the chip-level of overlapping headers due to the system-wide identical header spreading sequences. In addition, due to the concurrent nature of packet transmissions, header detection has to operate under heavy interference. As follows, immediately from the fact that $L_d > L_h$, this interference is mostly caused by data portions of competing packets. While in these two aspects similar to spread Aloha, in RP-CDMA, increasing the ratio L_d/L_h reduces collision effects.

We use spread Aloha as the baseline for our performance evaluations. The reasons for this are twofold. Firstly, spread Aloha is a very-well-known random, physical, and medium access control (MAC) protocol. Secondly, the RP-CDMA header essentially operates a spread Aloha system under very low load. Clearly, a thorough understanding of its behavior is substantial to the successful evaluation and proper modeling of RP-CDMA. If we assume that the packets' SINRs are such that power capture is impossible (in this context, the term *power capture* refers to the effect that if the power differential between two packets is very large, even if they are subject to header collisions, one packet may be recovered

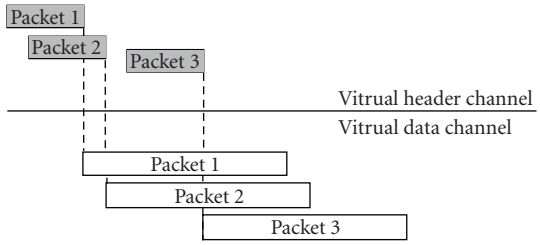

Figure 2: Traffic in the virtual header and data channels. Since $L_d > L_h$, interference for header detection is mostly generated by header/data (h/d) overlaps from other users' packets. This is shown in the case of the header of packet 3, which does not face (h/h) interference, but has to be captured in the presence of the data portions of packets 1 and 2.

successfully while only the weaker one is lost), we can express the probability for successful header detection as

$$p(h = \text{succ}) = \min\{p(h = \text{succ} \mid \text{coll}),\ p(h = \text{succ} \mid \text{inter})\}, \tag{8}$$

where $p(h = \text{succ} \mid \text{coll})$ and $p(h = \text{succ} \mid \text{inter})$ denote the probabilities for correct header detection under the header collision and interference limitation models, respectively (the probability of successful header detection is the minimum of the probability of success of two independent processes: successful detection under the collision and the interference assumption). In contrast to header detection, data detection in RP-CDMA is only a function of the interference resolution capabilities of the data detector with associated probability of correct detection $p(d = \text{succ} \mid \text{inter})$. Thus, the overall system throughput (S) of an RP-CDMA system can be found as

$$S_{\text{RP-CDMA}} = G \times p(h = \text{succ}) p(d = \text{succ} \mid \text{inter}), \tag{9}$$

where G denotes offered load in packets. Note that the notion of G directly implies that packets arrive in the transmitters queues at a rate of $\lambda = 1$ and are transmitted with probability $p(\text{trans}) = 1$. As a result, a load of $G = x$ packets translates directly into x active transmitters out of the overall network population.

We proceed to build a realistic performance model of RP-CDMA in a step-by-step fashion, starting with the header process. At first, we model spread Aloha under an imaginary *collision-only* assumption and transfer the results to the RP-CDMA header process. Next, we repeat this exercise but this time consider only interference. This gradual approach will later guide us to determine optimal parameter values as a function of RP-CDMA system load. We then investigate the performance of various multiuser receivers applied to the RP-CDMA data frame. Finally, we combine the results for the header (collision and interference limited) and data portions of the RP-CDMA system in Section 6.

4.1. Performance from a Collision Perspective. We now address the *header collision effects* by first investigating the behavior of spread Aloha and then use this understanding to model the RP-CDMA header process.

4.1.1. The Collision Limitation of Spread Aloha. In spread Aloha under the assumed system model (Section 2.3), a packet is lost if two or more packets overlap on the chip-level. Also, since the sequence is repeated for every bit, the collision vulnerable zone repeats L times throughout the packet duration in a packet of length L bits. We note that for every bit, a node has N possibilities to place the starting chip of its packet. We move on to express the conditional probabilities for packet survival in spread Aloha under the collision model, $\epsilon_{n,k}^{(\text{SA, coll})}$.

Let $u_i \geq 0$ denote the number of new packets in the ith chip, and note that when there are n active users,

$$u_1 + u_2 + u_3 + \cdots + u_N = n. \tag{10}$$

However, $\epsilon_{n,k}^{(\text{SA, coll})}$ is obtained by exploring all possible solutions to (10) and evaluating the ratio of the number of solutions where exactly k of the u_i's are equal to 1 over A_{tot}, the number of all possible solutions. This study, which is presented in the Appendix, leads to

$$\begin{aligned} \epsilon_{n,k}^{(\text{SA, coll})} &= \frac{A_k^{(\text{SA, coll})}}{A_{\text{tot}}^{(\text{SA, coll})}} \\ &= \frac{\binom{N}{k} \sum_{\max(0,m_{\min})}^{N-k-1} \binom{N-k}{m} A_m^{(\text{SA})}}{\binom{n+N-1}{n}}. \end{aligned} \tag{11}$$

As an example, in the case when $N = 10$ and $n = 5$, by using (11), we obtain

$$\widetilde{\mathbf{E}}^{(\text{SA, coll})} = \begin{pmatrix} 1 & 0 & 0 & 0 & 0 \\ 0 & 0.8182 & 0 & 0 & 0 \\ 0.4091 & 0 & 0.5455 & 0 & 0 \\ 0.1259 & 0.5035 & 0 & 0.2937 & 0 \\ 0.2248 & 0.1798 & 0.4196 & 0 & 0.1259 \end{pmatrix}. \tag{12}$$

Also here, the level of achievable QoS is $\eta = 0.56$. From our discussion in Section 3.2, we expect this system realization to be able to support at most

(i) 1 stable user with a maximum arrival rate of $\lambda = 1$,

(ii) 2 stable, homogeneous users with maximum arrival rates of $\lambda = 0.8182$,

(iii) 3 stable, homogeneous users with maximum arrival rates of $\lambda = 0.5455$,

(iv) ....

In Table 1, we further investigate the performance of spread Aloha in the collision model by presenting η as N and K vary. There, we show by how much N needs to be increased as K grows to maintain a certain level of QoS. In the following, we use the obtained $\eta \approx 0.92$ in the case when $K = 5$ and $N = 100$ as our baseline for comparison. As we double the number of users to $K = 10$, to maintain the same level of QoS, N needs to be increased to $N = 400$. Finally, as we further increase K to $K = 20$, compared to the baseline value of $N = 100$,

Table 1: Spread Aloha, collision behavior as N and K vary.

	$\eta = \zeta/K$		
	$K = 5$	$K = 10$	$K = 20$
$N = 100$	0.926	0.7488	0.443
$N = 200$		0.8575	0.462
$N = 400$		0.925	0.748
$N = 800$			0.856
$N = 1600$			0.923

a multiplication of the spreading gain by a value of 2^4 is required to maintain $\eta \approx 0.92$. One can see that any doubling in the number of users K requires a quadratical increase in signaling dimensions N to maintain identical collision performance. This illustrates a fundamental problem of spread Aloha. Since it is impractical to increase the spreading gain dramatically because of the scarce wireless resource and also because of transceiver complexity, spread Aloha is limited to systems with a small number of active users. While basically, the RP-CDMA header process also relies on the principles of spread Aloha; given identical resources (i.e., a certain spreading gain N), RP-CDMA allows to improve ζ by a factor of χ which is a function of L_d/L_h, such that $\zeta_{\text{RP-CDMA}} = \chi \times (\zeta_{\text{S-ALOHA}})$, and $\chi > 1$ grows with L_d/L_h.

4.1.2. The Collision Limitation of RP-CDMA Header Detection. For convenience, we refer to this scenario as *RP-CDMA case (B)* to be consistent with [31] (there, *RP-CDMA case (A)* refers to the scenario when any header overlap automatically leads to the loss of all involved packets, i.e., the classical Aloha assumption). In *RP-CDMA case (B)*, we assume that the receiver always has a sufficient number of parallel header detectors and packets are only lost due to collisions on the channel. To derive the conditional probabilities $\epsilon_{n,k}^{(B)}$ for this case, we note that only headers that actually overlap are subject to the spread Aloha mechanism. Hence,

$$\epsilon_{n,k}^{(B)} = \sum_{|\mathcal{H}|=n-k}^{n} \epsilon_{n,n-|\mathcal{H}|}^{a} \epsilon_{|\mathcal{H}|,k-(n-|\mathcal{H}|)}^{b}, \tag{13}$$

where ϵ^a and ϵ^b represent the probabilities for correct and incorrect header detection due to collisions. Furthermore, $|\mathcal{H}|$ denotes the size of the set of the overlapping headers. For the evaluation of this equation, we recall that generally, the number of solutions of a function of the form shown in (13) in n variables is $O(2^n)$. As a result, an explicit computation of each individual solution for large values of N, n, and L_d/L_h is computationally prohibitive. In the following, we thus restrict our investigations to the cases where n, N, and L_d/L_h are relatively small. For larger networks, we resort to system-simulations for performance evaluation.

A study of (13) in the case when $N_d = N_h = 10$, $L_d/L_h = 10$, and $n = 5$ results in the corresponding modified multipacket reception matrix:

$$\widetilde{\mathbf{E}}^{(B)} = \begin{pmatrix} 1 & 0 & 0 & 0 & 0 \\ 0 & 0.9669 & 0 & 0 & 0 \\ 0.0930 & 0 & 0.9050 & 0 & 0 \\ 0.0075 & 0.1688 & 0 & 0.8206 & 0 \\ 0.0139 & 0.0164 & 0.2476 & 0 & 0.7215 \end{pmatrix}, \tag{14}$$

and $\eta^{(B)} = 0.88$. When we compare $\eta^{(\text{SA,coll})}$ and $\eta^{(B)}$, it is clear that from a mere collision perspective, *RP-CDMA case (B)* will deliver far better QoS.

4.2. The Performance of RP-CDMA and Spread Aloha from an Interference Perspective. In the previous sections, we assumed that RP-CDMA as well as spread Aloha only face collision effects. We now more closely investigate the negative impact of interference on system performance. Our investigation includes the characteristics of header as well as data detection in RP-CDMA. We recall that the differentiation into header and data detection in RP-CDMA is necessary, since for header recovery, packet-specific timing information is not yet available and thus header detection has to rely on matched filtering. As soon as timing has been established, advanced multiuser techniques are available for the remainder of the packet. As far as spread Aloha is concerned, multiuser techniques cannot be used to improve performance because of its restrictive collision behavior (see [32–34]). Assuming that all transmitters in the network employ power control, the powers at the receiver ($P_{\text{RX},j}$) are equal, and, therefore, $P_{\text{RX},j} = P$ for all j, $j = 1, \ldots, K$.

4.2.1. Performance of Spread Aloha under Interference Effects. Before addressing RP-CDMA from an interference perspective, we first determine the achievable performance under spread Aloha. From [35, 36], the received SINR, Γ for a packet j with a matched filter receiver is given by

$$\Gamma_j^{(\text{mf})} = \frac{P_j}{\sigma^2 + (1/N)\sum_{i=1, i\neq j}^{n} P_i}, \tag{15}$$

where P_j is the power of the jth user, and we assumed n active packets in the system at the time packet $j$are transmitted. As we can see, the interfering powers are scaled down by the spreading factor (N). From (15), we can directly compute the maximum number of successfully detectable packets n_{crit} given some detection threshold γ as

$$\begin{aligned} \gamma &\leq \frac{P}{\sigma^2 + ((n_{\text{crit}} - 1)/N)P}, \\ n_{\text{crit}} &\leq \left(\frac{P - \sigma^2\gamma}{\gamma P}\right)N + 1, \end{aligned} \tag{16}$$

such that

$$\epsilon_{n,k} = \begin{cases} \epsilon_{n,n} = 1, & n \leq n_{\text{crit}}, \\ \epsilon_{n,0} = 1, & \text{otherwise}, \end{cases} \tag{17}$$

which fully defines the multipacket reception matrix $\mathbf{E}$ since the elements in the rows of $\mathbf{E}$ must sum to 1.

As an example, with $P/\sigma^2 = 10\,\text{dB}$, a detection threshold of $\gamma = 3\,\text{dB}$, a maximum number of active users $n = 6$, and a spreading gain of $N_{\text{SA}} = 10$, the modified multipacket reception matrix $\widetilde{\mathbf{E}}$ has the following form:

$$\widetilde{\mathbf{E}}^{(\text{SA,inter})} = \begin{pmatrix} 1 & 0 & 0 & 0 & 0 & 0 & 0 \\ 0 & 1 & 0 & 0 & 0 & 0 & 0 \\ 0 & 0 & 1 & 0 & 0 & 0 & 0 \\ 0 & 0 & 0 & 1 & 0 & 0 & 0 \\ 0 & 0 & 0 & 0 & 1 & 0 & 0 \\ 0 & 0 & 0 & 0 & 0 & 0 & 0 \end{pmatrix}. \tag{18}$$

From another angle, since the nonzero elements in $\mathbf{\Lambda}$ are sufficient for stability analysis, we have

$$\mathbf{\Lambda} = [\underbrace{1, 1, \ldots, 1}_{n_{\text{crit}}=5}, 0, \ldots]. \tag{19}$$

In contrast to the view motivated by chip-level collisions in Section 4.1.1, here when doubling K, doubling N results in a linear increase in the number of detectable packets. Essentially, *with perfect power control, Spread Aloha is in fact collision rather than interference limited* (see also [32–34]).

4.2.2. Performance of RP-CDMA Header Detection under Interference Effects. Because of its packet structure, header detection in RP-CDMA faces interference from header/header ((h/h)) and header/data ((h/d)) overlaps. As a consequence, since interference is dominated by (h/d) overlaps as outlined in Figure 2, *from an interference perspective*, distributed access control, such as carrier sense multiple access with collision avoidance (CSMA/CA) on the header frame, is unlikely to significantly improve system performance.

For simplicity, in the following, we refer to the behavior of RP-CDMA header detection under equal power users as *RP-CDMA, case (C)*. In addition to perfect power control, we allow the nodes to increase the header transmission power over the data transmission power to increase the probability for correct header detection. Thus, to determine the level of multiaccess interference, we need to investigate the number of packet overlaps in both virtual channels as a function of L_d/L_h. For successful header detection, we require that the total interference caused by overlapping (h/h) and (h/d) portions is less than some threshold γ. We define the two supporting sets: (i) $\mathcal{H}$: the set of (h/h) overlaps, and (ii) $\mathcal{D}$: the set of (h/d) overlaps, and accordingly modify (15) as

$$\Gamma_j^{(\text{mf})} = \frac{P_{h,i}}{\sigma^2 + (1/N_h)\sum_{\mathcal{H}} P_{h,k} + (1/N_d)\sum_{\mathcal{D}} P_{d,j}}, \tag{20}$$

where j refers to the packet under observation, while P_h and P_d represent the transmission powers of the header and data portions of the packet, respectively. In order to calculate the corresponding $\epsilon_{n,k}^{(C)}$, we note that the sizes of those sets, $|\cdot|$, given n active packets, can be approximated by

$$\begin{aligned} |\mathcal{H}| &\approx E\left[\frac{h}{h}\right] = n\frac{L_h}{L_d}, \\ |\mathcal{D}| &\approx E\left[\frac{h}{d}\right] = n\left(1 - \frac{L_h}{L_d}\right). \end{aligned} \tag{21}$$

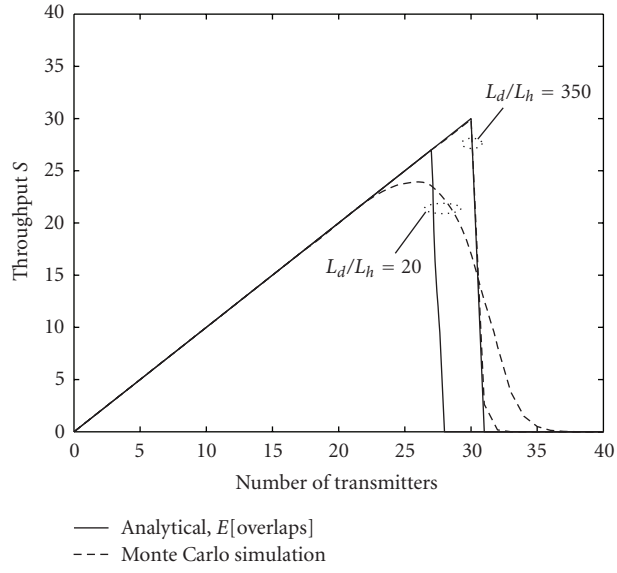

Figure 3: Comparison of the approximations in (21) to Monte Carlo simulations of the header detection limitation in the case of equal receive SINRs of $P_h/\sigma^2 = 15\,\text{dB}$ and $P_d/\sigma^2 = 10\,\text{dB}$, spreading gain $N = 20$ and different ratios $L_d/L_h = 20$ and $L_d/L_h = 350$.

Figure 3 shows the quality of our approximations for two values of $L_d/L_h = 20$ and $L_d/L_h = 350$ with $N_h = N_d = 20$ compared to Monte Carlo simulations of system performance. Even for the smaller value, expressing the number of overlapping headers and data frames in terms of their expected value leads only to a slight overevaluation of system throughput, S.

Substituting (21) in (20), noting that successful detection of the header requires $\Gamma_j^{(\text{mf})} > \gamma$ and dropping the user index for simplicity, we get

$$n_{\text{crit}} \leq \frac{(P_h/\gamma) - \sigma^2}{P_h L_h/N_h L_d + (P_d/N_d)(1 - L_h/L_d)} + 1. \tag{22}$$

The elements in $\mathbf{E}$ can then be found by applying (17). As an example, when the header and data signal-to-noise ratios are $P_h/\sigma^2 = P_d/\sigma^2 = 10\,\text{dB}$, the header detector threshold $\gamma = 3\,\text{dB}$, $N_h = N_d = 10$, and $L_d/L_h = 60$, and the maximum number of transmitters in the network is $K = 7$, the modified multipacket reception matrix $\widetilde{\mathbf{E}}^{(C)}$(resp., $\mathbf{\Lambda}$) have the form shown in (18) and (19) with $n_{\text{crit}} = 5$. Essentially, in this case, RP-CDMA header detection is limited by (h/d) interference. However, as we increase $P_h/P_d = 0\,\text{dB}$ to $P_h/P_d = 3\,\text{dB}$, $\widetilde{\mathbf{E}}^{(C)}$ becomes full rank with $n_{\text{crit}} = 7$. We want to emphasize that this method of improving system performance is unique to RP-CDMA and impractical in spread Aloha systems. The reason is as follows: the RP-CDMA header makes up only a small fraction of the overall RP-CDMA packet, hence, increasing its transmission power over the transmission power of the data frame makes it more robust against multiuser interference generated by the data frames of overlapping packets. Of course, one has to ensure that the interference generated by the now-stronger headers still allows for successful recovery of the data portions of

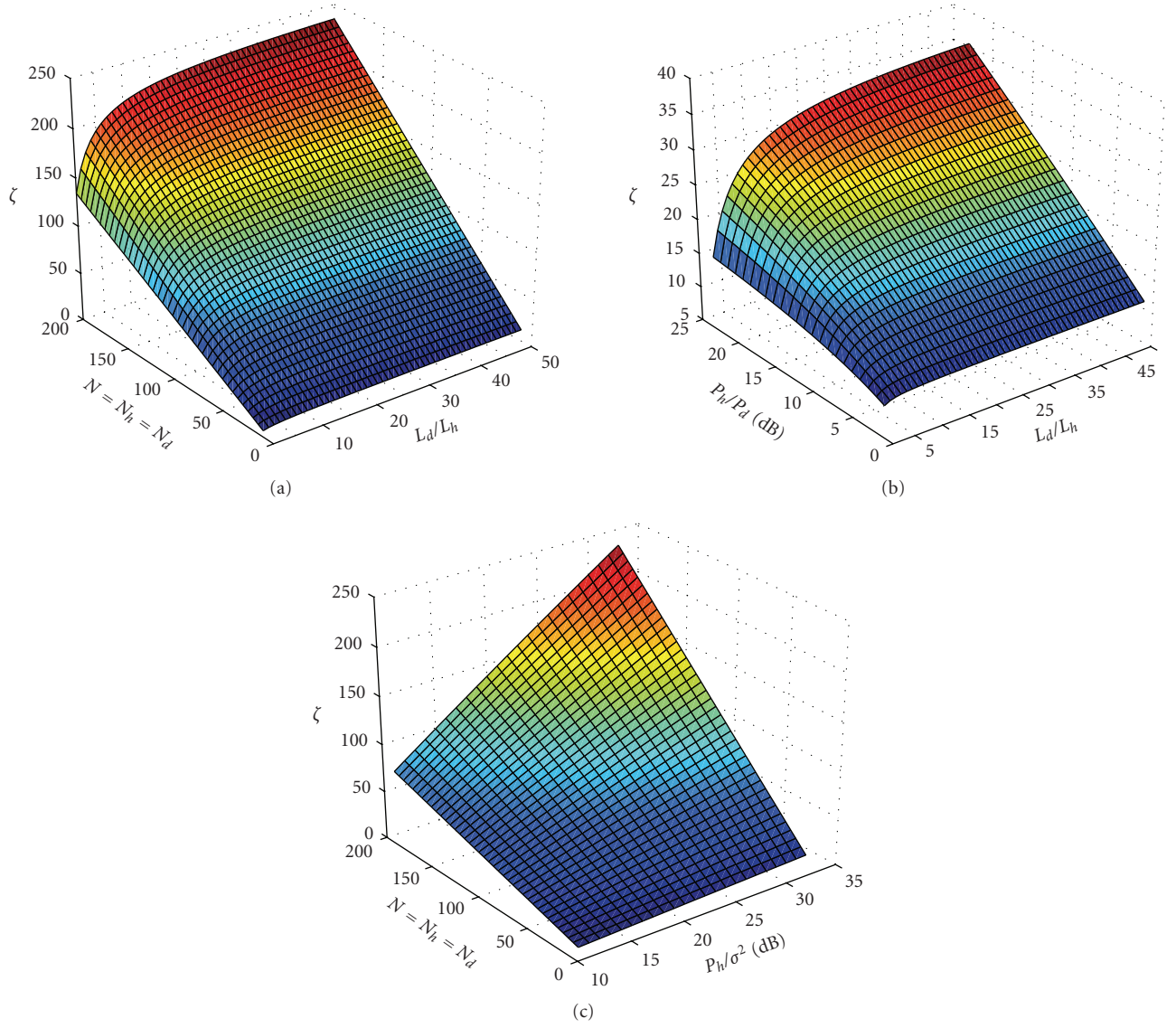

Figure 4: Performance analysis of RP-CDMA header detection, equal receive powers, interference limit only. (a) ζ for fixed header and data transmission SINRs of $P_h/\sigma^2 = 15$ dB, $P_d/\sigma^2 = 10$ dB, and detection threshold $\gamma = 3$ dB as a function of the header and data spreading gains $N = N_h = N_d$ and the data to header ratio L_d/L_h. (b) ζ for fixed $N_h = N_d = 20$ and varying P_h/σ^2 for a fixed $P_d/\sigma^2 = 10$ dB. (c) ζ for fixed $L_d/L_h = 25$ and fixed data transmission SINR of $P_d/\sigma^2 = 10$ dB.

competing users. In spread Aloha, any increase in packet transmission power very strongly increases the interference for other packets and can thus have a disastrous effect for other users.

Finally, in Figure 4, we investigate the performance of the header detection process as a function of the spreading gains N_h and N_d, P_h/P_d, as well as L_d/L_h. We assume a header length of $L_h = 50$ bits, which allows for reliable timing recovery as interference increases [37]. Figure 4(a) presents variations of ζ as $N = N_h = N_d$ and L_d/L_h vary and $P_h/\sigma^2 = 15$ dB, $P_d/\sigma^2 = 10$ dB, and $\gamma = 3$ dB. We observe that while increasing $N = N_h = N_d$ offers a monotonic increase in the number of detected headers, performance increases only slowly when we increase L_d/L_h alone. Figure 4(b) presents similar results when we fix $N = N_h = N_d = 20$ and $P_d/\sigma^2 = 10$ dB and vary P_h/σ^2. Increasing P_h/σ^2 offers a monotonic increase in the number of detected headers, while for a given P_h/σ^2 and P_d/σ^2, increasing L_d/L_h beyond $L_d/L_h \approx 25$ offers little performance gain. Finally, in Figure 4(c), we observe that for fixed $L_d/L_h = 25$ and $P_d/\sigma^2 = 10$ dB, increasing either or both, P_h and N, improves system performance.

As a result of the discussion in Figure 4, we conclude that there is a point after which RP-CDMA becomes *interference limited* instead of *header collision limited*, and increasing L_d/L_h does not improve performance noticeably. This point depends on the available header detection technology as well as on N_h, respectively, L_dN_d/L_hN_h and P_h/P_d. As an example, with $\gamma = 3$ dB, little performance as a function of L_d/L_h can be gained once $L_d/L_h > 25$. In such cases, it is beneficial to increase N_h separately from N_d such that a

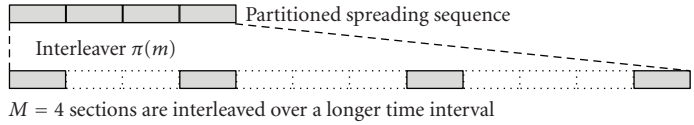

Figure 5: Partitioned and interleaved spreading for CDMA, $M = 4$.

maximum effective ratio of header to data *on the channel* of $N_d L_d / L_h N_h \approx 25$ is maintained.

5. The Performance of RP-CDMA Data Detection

In the following, we investigate the performance of RP-CDMA data reception with the matched filter, the decorrelator, the MMSE, as well as partitioned spreading demodulation. We proceed to give a brief overview of the various multiuser receiver technologies.

5.1. Data Detection with the Matched Filter. Data detection in RP-CDMA with a matched filter receiver leads to the performance of spread Aloha, which was evaluated in Section 4.2.1.

5.2. Data Detection with the Decorrelator. The decorrelating receiver inverts the channel to completely eliminate interference. This results in a loss of energy for each user, depending on the user population. Interference no longer depends on the power of other users, and the SINR for packet j after the decorrelating receiver reduces to SINR [35]:

$$\Gamma_j^{(\mathrm{deco})} = \frac{P_j}{\sigma^2} \frac{N - n + 1}{N}. \tag{23}$$

In the equal power case, we can rewrite (23) and solve for the maximum number of detectable packets (n_{crit}) directly as

$$\gamma \leq \frac{P}{\sigma^2} \frac{N - n_{\mathrm{crit}} + 1}{N}. \tag{24}$$

Rearranging this result, we get

$$n_{\mathrm{crit}} \leq N + 1 - \frac{\gamma \sigma^2 N}{P}, \tag{25}$$

and $\epsilon_{n,k}^{(\mathrm{deco})}$ follows from (17). In the case when $N = 10$, $P/\sigma^2 = 10\,\mathrm{dB}$, $\gamma = 3\,\mathrm{dB}$, the corresponding $\widetilde{\mathbf{E}}^{(\mathrm{deco})}$ and $\mathbf{\Lambda}^{(\mathrm{deco})}$ once more have the forms shown in (18) and (19) with $n_{\mathrm{crit}} = 9$.

5.3. Data Detection with the MMSE Filter. The MMSE establishes a filter to minimize the mean-square error caused by noise and the multiaccess interference. For the MMSE receiver, a given packet j will be received successfully if its power P_j satisfies [35]

$$\gamma \leq \frac{P_j}{\sigma^2 + (1/N) \sum_{i=1, i \neq j}^{n} \left(P_j P_k / (\gamma P_k + P_i) \right)}. \tag{26}$$

Under perfect power control, (26) reduces to

$$\gamma \leq \frac{P}{\sigma^2 + \left((n_{\mathrm{crit}} - 1)/N \right) \left(P^2 / (\gamma P + P) \right)}. \tag{27}$$

This can be rearranged as

$$n_{\mathrm{crit}} \leq N \left(\frac{1 + \gamma}{\gamma} - \frac{1 + \gamma}{P \sigma^2} \right). \tag{28}$$

In the case when $N = 10$, $P/\sigma^2 = 10\,\mathrm{dB}$, and $\gamma = 3\,\mathrm{dB}$, here also, $\widetilde{\mathbf{E}}^{(\mathrm{mmse})}$ and $\mathbf{\Lambda}^{(\mathrm{mmse})}$ have the form shown in (18) with $n_{\mathrm{crit}} = 13$.

5.4. Data Detection with Partitioned Spreading. Partitioned spreading is a recently proposed technique which utilizes the benefits of interleaving and iterative receiver processing. To make this paper more self-contained, we summarize the findings already presented in [36, 38, 39]. In partitioned spreading, the spreading waveform for each symbol is partitioned into M sections. The different sections are interleaved over a number of section intervals, as shown in Figure 5, and the gaps in the figure are filled by the partitions from other symbols. The interleaving function $\pi(m)$ is to spread partitions of the original chip waveform such that interfering partitions belong to statistically independent symbols and no correlation can build up. The function of this interleaver is analogous to that used for turbo codes [40] and the received signal with K active users is given by

$$y(t) = \sum_{k=1}^{K} \sqrt{P_k} x_k(t) + n(t), \tag{29}$$

where $x_k(t)$ is the signal from user k, $n(t)$ is zero mean white Gaussian noise with double-sided noise power spectral density $\sigma^2 = N_0/2$.

The receiver operates with a number of stages (or iterations). The first stage is a conventional matched filter receiver. Due to the interleaving, each partition of the spreading waveform is individually filtered by a corresponding energy-normalized matched filter. Assuming that synchronization has been accomplished, the output signal after the matched filter of symbol l and partition m is given by

$$z_{k,l,m} = \sqrt{\frac{P_k}{M}} b_{k,l} + I_{k,l,m} + n_{k,l,n}, \tag{30}$$

where $b_{k,l}$ is the (binary) symbol of user k at position l, $n_{k,l,n}$ is white noise sample with power σ^2, and $I_{k,l,m}$ is interference from the other user, whose prefilter signal is given by

$$I_k(t) = \sum_{\substack{k'=1 \\ k' \neq k}}^{K} \sqrt{P_{k'}}\, x_{k'}(t). \tag{31}$$

Simply, adding all the different matched partitions, that is, $\sum_{m=1}^{M} z_{k,l,m}$, leads to the conventional matched filter receiver for CDMA. Instead, we derive the a posteriori probability for the transmitted bit $b_{k,l}$ from each received sample $z_{k,l,m}$, given by

$$\Pr(b_{k,l} = \pm 1 | z_{k,l,m}) = \kappa \exp\left(-\frac{\left(z_{k,l,m} \pm \sqrt{P_k}/M\right)^2}{2\sigma_k^2} \right), \tag{32}$$

where we have used the fact that $I_{k,l,m}$ rapidly assumes a Gaussian distribution as K becomes large. This is true for large K and N under mild conditions on the powers P_k (see, e.g., [41]). The variance σ_k^2 is that of the joint interference and noise, that is, of $I_{k,l,m} + n_{k,l,n}$.

Since the different partitions have to agree on the transmitted bit, we compute the cumulative probabilities of $b_{k,l}$ as

$$\begin{aligned} &\Pr\left(b_{k,l} = \pm 1 | z_{k,l,1}, \ldots, z_{k,l,M}\right) \\ &\quad = \kappa \exp\left(-\frac{1}{2\sigma_k^2} \sum_{m=1}^{M} \left(z_{k,l,m} \mp \sqrt{\frac{P_k}{M}} \right)^2 \right). \end{aligned} \tag{33}$$

From (33), we can compute a *soft-bit estimate* of $b_{k,l}$ as

$$\begin{aligned} \widetilde{b}_{k,l} &= \ln\left(\Pr(b_{k,l} = 1 | z_{k,l,1}, \ldots, z_{k,l,M})\right) \\ &\quad - \ln\left(\Pr(b_{k,l} = -1 | z_{k,l,1}, \ldots, z_{k,l,M})\right) \\ &= \tanh\left(\frac{\sqrt{P_k}}{\sqrt{M}\sigma_k^2} \sum_{m=1}^{M} z_{k,l,m} \right). \end{aligned} \tag{34}$$

Such soft-bits are now used to reduce the mutual interference. In a subsequent decoding step, soft-bits from the previous step are used to cancel part of the signal interference for each user k, given a next-stage received signal $y_k^{(i+1)}(t)$ where part of the interference has been canceled using reconstructed interference signals modulated by the soft-bits

$$\widetilde{b}_{k',l,m}^{(i)} = \tanh\left(\frac{\sqrt{P_k}}{\sqrt{M}\sigma_{i,k'}^2} \sum_{\substack{m'=1 \\ m' \neq m}}^{M} z_{k',l,m'} \right), \tag{35}$$

where $\sigma_{i,k'}^2$ is the residual variance of $I_{k',l,m} + n_{k',l,n}$ at stage i. The initial variance is $\sigma_{0,k'}^2 = (K-1)/N + \sigma^2$.

We now calculate the variance $\sigma_{i,k'}^2$ of the interference and noise at iteration stage i. Due to the random spreading, the interference power of a user k' on the postmatched filter signal of user k is given by $P_{k'}\sigma_{i,k',b}^2/N$, where $\sigma_{i,k',b}^2 = E(b_{k',l} - \widetilde{b}_{k',l,m}^{(i)})^2$. Adding up all the contributions, we obtain

$$\sigma_{i,k}^2 = \sum_{\substack{k'=1 \\ k' \neq k}}^{K} \sigma_{b,i,k'}^2 \frac{P_{k'}}{N} + \sigma^2. \tag{36}$$

For large numbers of users K, and under some mild conditions on the powers $P_{k'}$ [42], the interference variance becomes independent of k as the contribution of the kth term vanishes, and is given by

$$\sigma_i^2 = \sum_{k'=1}^{K} \sigma_{b,i,k'}^2 \frac{P_{k'}}{N} + \sigma^2. \tag{37}$$

How ever, $\sum_{m'=1, m' \neq m}^{M} z_{k',l,m'}$ has mean and variance equal to $P_k(M-1)/(M\sigma_i^2)$ [38], and we can write

$$\widetilde{b}_{k',l,m}^{(i)} = \tanh\left(\frac{M-1}{M}\frac{P_{k'}}{\sigma_i^2} + \sqrt{\frac{M-1}{M}\frac{P_{k'}}{\sigma_i^2}}\,\xi \right), \tag{38}$$

where $\xi \sim \mathcal{N}(0,1)$. Now,

$$\begin{aligned} E\left(b_{k',l} - \widetilde{b}_{k',l,m}^{(i)}\right)^2 &= E(1 - \tanh(b^2 + b\xi))^2; \\ b &= \sqrt{\frac{M-1}{M}\frac{P_{k'}}{\sigma_i^2}}. \end{aligned} \tag{39}$$

Equation (39) has no closed-form solution, but the following bounds are tight [43]:

$$\begin{aligned} &E(1 - \tanh(b^2 + b\xi))^2 \\ &\quad \leq \min\left\{ \frac{1}{1+b^2}, \pi Q(b) \right\} = \begin{cases} \dfrac{1}{1+b^2}, & b < 1, \\ \pi Q(b), & b \geq 1. \end{cases} \end{aligned} \tag{40}$$

The assumption in (38) is admissible as long as the interleaving of partitions is sufficient to ensure no or only minimal correlation among successive soft-bits used for cancellation. This is usually quickly achieved even with moderate levels of spreading in the order of a few hundred symbols. Using (37) and the bound (40), the variance evolution follows:

$$\begin{aligned} \sigma_i^2 \leq \sum_{k=1}^{K} \frac{P_k}{N} \min\Bigg(&\frac{1}{1 + ((M-1)/M)\left(P_k/\sigma_{i-1}^2\right)}, \\ &\pi Q\left(\sqrt{\frac{M-1}{M}\frac{P_k}{\sigma_{i-1}^2}} \right) \Bigg) + \sigma^2, \end{aligned} \tag{41}$$

where the summation is over all active users, and M denotes the number of partitions. A packet j will be successfully decoded if after iteration i, its SINR satisfies

$$\Gamma_j^{(\mathrm{ps})} = \frac{P_j}{\sigma_i^2} \geq \gamma.$$

In our well-used example with $P/\sigma^2 = 10\,\mathrm{dB}$ and $N = 10$, when we choose $M = N/2 = 5$ and detection threshold $\gamma = 3\,\mathrm{dB}$, partitioned spreading achieves a maximum of $n_{\mathrm{crit}} = 12.5$ and the modified multipacket reception matrix remains unchanged from its triangular form in (18) with $n_{\mathrm{crit}} = 12$.

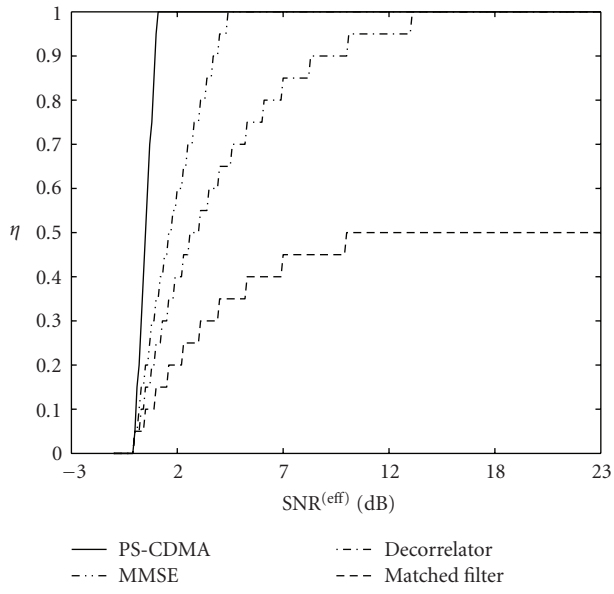

FIGURE 6: Comparison of the achievable $\eta = f(\text{SINR}^{(\text{eff})})$ for the different receivers, equal power, $\text{SINR}^{(\text{eff})} = \text{SINR} - \gamma$. Spreading gain for all reception methodologies of $N = 20$ with detection thresholds of $\gamma = 3$ dB, partitioning factor $M = N/4$. $\eta = 1$ reflects a *fully loaded system*, that is, optimal performance.

5.5. Comparison of the Various Multiuser Receivers. In Figure 6, we compare the maximum η as a function of the effective SINR which can be presented as $\eta = f(\text{SINR}^{(\text{eff})})$, $\text{SINR}^{(\text{eff})} = (\text{SINR} - \gamma)$, achievable with the various receivers presented above. We assume a spreading gain of $N = 20$ and detection thresholds of $\gamma = 3$ dB. We recall that $\eta = 1$ reflects a *fully loaded system*, that is, the optimal multiple access system. For $\text{SINR}^{(\text{eff})} \geq 1$ dB, partitioned spreading allows for such a fully loaded system with one user per dimension, making it the most spectrally efficient receiver. Also, $\eta^{(\text{ps})}$ is followed by the MMSE which achieves $\eta^{(\text{mmse})} = 1$ at an $\text{SINR}^{(\text{eff})} \approx 4.5$ dB and the decorrelator which requires a significantly higher-powered environment of approximately 13 dB for $\eta^{(\text{dc})} = 1$. As expected from [35], the matched filter receiver is unable to achieve $\eta = 1$, and $\eta^{(\text{mf})} \ll 1$.

6. Network Simulations

We now simulate RP-CDMA in base station centric networks with the various detectors introduced and evaluated above. We investigate throughput as well as average queue sizes. Again, our baseline for comparison is spread Aloha. From Section 4, we recall that the performance of RP-CDMA—especially when partitioned spreading detection is applied to the data frame—is critically determined by the interference suppression capabilities of the header detection stage rather than by the header collision process.

We assume that the accessing terminals are located in a cell and transmit packets to a central base station according to Section 2.4. For our analysis of the nodes' queues, we introduce Ω, defined as the average growth rate of the queues per (re-)transmission attempt. In general, the value of Ω lies between $\Omega = 0$, indicating that every transmission was a success, and $\Omega = 1$, indicating that no packet could be transmitted successfully during a transmission attempt, hence maximum queue buildup. In the following subsections, we validate through simulations our earlier claim made in Section 3.2, where we stated that $\boldsymbol{\Lambda}$ presents the upper limit of the vector of arrival rates $\boldsymbol{\lambda}$ which leads to network stability. In contrast to previous sections, in our network simulations, the *collision behavior* of RP-CDMA as well as spread Aloha captures their intended asynchronous mode of operation. Once more, we envision the application of strong error-correcting codes in the data stages, thus the modeling of asynchronous packet overlap is not necessary for the systems' *interference behavior*. To determine the value for L_d/L_h, we turn our attention to Internet2 traffic. There, the packet size is trimodally distributed with lengths of $L = 50$, $L = 500$, and $L = 1500$ bytes and respective probabilities of occurrence of $p(L = 50) = 0.5$, $p(L = 500) = 0.4$, and $p(L = 1500) = 0.1$ [44]. Assuming a header length of $L_h = 50$ bits, we have $E[L_d/L_h] = 60$. Clearly, with these figures and from a mere collision perspective, RP-CDMA promises great improvements over spread Aloha, possibly approaching the performance of a fully access controlled system, as was also concluded in [6, 45, 46]. In our model, we assume that any packet that exceeds the detection threshold will be decoded, respectively, detected successfully.

We now demonstrate that $\boldsymbol{\Lambda}$ allows us to find a vector of stable arrival rates $\boldsymbol{\lambda}$. From Section 4, for the parameters chosen for spread Aloha in Figure 7, the vector of the diagonal elements of the resulting effective modified multipacket reception matrix ($\boldsymbol{\Lambda}^{(\text{SA,eff})}$) are

$$\begin{aligned}\boldsymbol{\Lambda}^{(\text{SA,eff})} &= \min\left(\boldsymbol{\Lambda}^{(\text{SA,coll})}, \boldsymbol{\Lambda}^{(\text{SA,inter})}\right)\\ &= [1.000, 0.905, 0.740, 0.547, 0.365, 0.219, 0.118, 0.057],\end{aligned} \tag{42}$$

and all other elements are zero. In Figure 7, we show (a) system throughput S, and (b) the rate of the growth of the queue size, Ω, for three different realizations of $\boldsymbol{\lambda}$: (i), $\boldsymbol{\lambda} = \mathbf{1}$, (ii), $\boldsymbol{\lambda} = \Lambda_n$, where $n \leq K$ denotes the desired number of stable users, and (iii), $\boldsymbol{\lambda} = \Lambda_n + \epsilon$, where $\epsilon = 10\%$ of the corresponding entries in $\boldsymbol{\Lambda}$. We chose a rather large value of ϵ to accelerate the increase in Ω, since as the number of active transmitters increases, the respective elements in $\boldsymbol{\Lambda}$ decrease in value quickly, making transmissions less likely. The case when $\boldsymbol{\lambda} = \mathbf{1}$ results in maximum throughput for the system—but leads to queue instability. When $\boldsymbol{\lambda} = \Lambda_n$ as seen in (b), the average growth of the queue sizes remains $\Omega = 0$ for all loads. However, the throughput dropped significantly, achieving a maximum of $S_{\boldsymbol{\lambda}=\boldsymbol{\Lambda}} \approx 2.2$ at a load of $G = 3$ compared to $S_{\boldsymbol{\lambda}=\mathbf{1}} \approx 4.3$ at $G = 8$. As $\boldsymbol{\lambda}$ is increased to $\boldsymbol{\lambda} = \Lambda_n + \epsilon$, throughput slowly increases towards $S_{\boldsymbol{\lambda}=\mathbf{1}}$, however, queues begin to build up.

From the above observations, we come to the conclusion that $\boldsymbol{\Lambda}$ can be used to predict the efficiency of a multiaccess

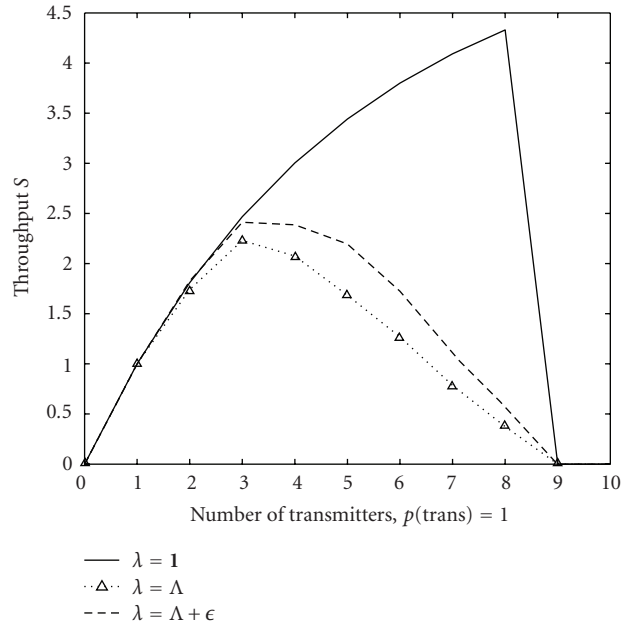

(a)

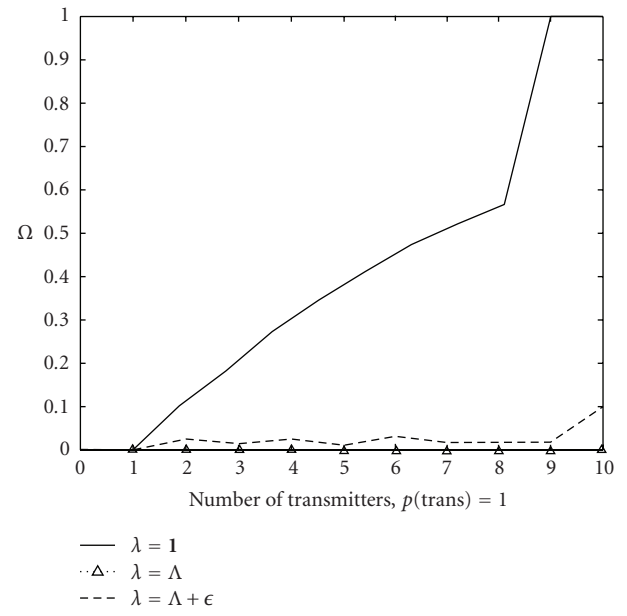

(b)

Figure 7: Spread Aloha, comparison of three different arrival rates, $\boldsymbol{\Lambda} = \mathbf{1}, \boldsymbol{\lambda} = \Lambda_n$, and $\boldsymbol{\lambda} = \Lambda_n + \epsilon$, where $\epsilon = 10\%$ of the corresponding value in $\boldsymbol{\Lambda}$. (a) network throughput and (b), Ω as functions of the network load, G. $N = 20$, $P_{\text{SA}}/\sigma^2 = 12\,\text{dB}$, detection threshold $\gamma_{\text{SA}} = 3\,\text{dB}$. Achieving maximum throughput $S = S_{\max}$ comes at the expense of increasing Ω.

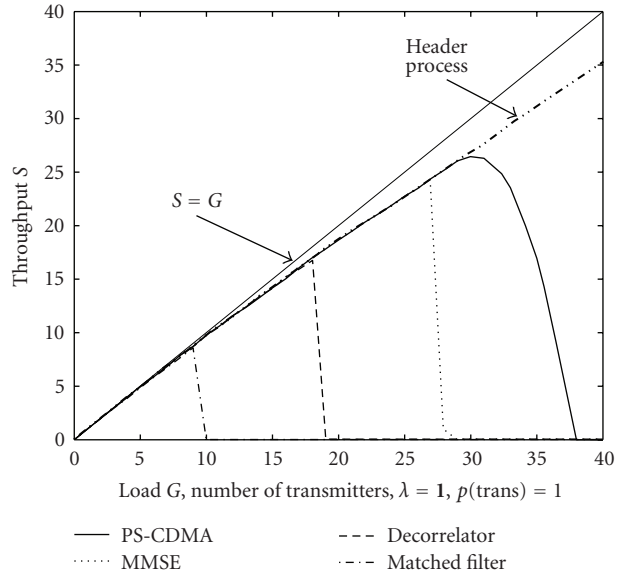

(a)

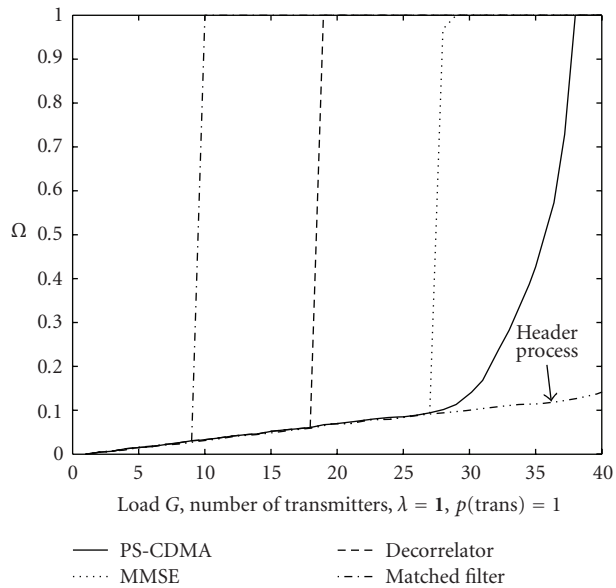

(b)

Figure 8: (a) Network throughput and (b), Ω as a function of the network load, G. $N_h = N_d = 20$, trimodal packet sizes and $L_h = 50$ bits such that $E[L_d/L_h] = 60$. $P_d/\sigma^2 = 12\,\text{dB}$, $P_h/\sigma^2 = 15\,\text{dB}$. Detection thresholds of $\gamma_d = 3\,\text{dB}$, $\gamma_h = 1\,\text{dB}$. For partitioned spreading, $M = N_d/2 = 10$.

system. The less a given $\widetilde{\mathbf{E}}$ equals $\mathbf{I}$—as indicated by the difference between ζ and the number of users n—the bigger the difference between $S_{\boldsymbol{\lambda}=\mathbf{1}}$ and $S_{\boldsymbol{\lambda}=\boldsymbol{\Lambda}}$. In other words, such systems are spectrally inefficient, and since the stable arrival rates are low, they should be restricted to low-traffic networks. On the other hand, the more $\widetilde{\mathbf{E}}$ approaches $\mathbf{I}$, the less the difference between $S_{\boldsymbol{\lambda}=\mathbf{1}}$ and $S_{\boldsymbol{\lambda}=\boldsymbol{\Lambda}}$. This means that the network is able to support a large and very active user base, allowing the system to best harness its assigned spectral resources.

We now compare these results to the achievable performance under RP-CDMA. Figure 8 shows simulation results in the case when the header and data SINRs are $P_h/\sigma^2 = 15\,\text{dB}$ and $P_d/\sigma^2 = 12\,\text{dB}$, resulting in $P_h/P_d = 3\,\text{dB}$.

Furthermore, the header and data spreading gains are $N_h = N_d = 20$, we assume trimodal packets with a header size of 50 bits and a data detection threshold of $\gamma_d = 3$ dB as in the case of spread Aloha presented above. For data detection, we employ all multiuser detectors discussed in Section 4. For header detection, we assume a threshold for matched filtering of $\gamma_h = 1$ dB. Choosing a lower threshold is possible in RP-CDMA, since the header is merely used for timing and code-ID recovery with resulting low transmission rates. While the value of 1 dB has been chosen somewhat arbitrarily, we note that even lower values might be possible in practice (see [47]) for a discussion on the fundamental limits of detection in the low SINR regime. Like before, Figure 8(a) shows achieved throughput (S) and Figure 8(b) depicts Ω, both versus offered load G. Starting with Figure 8(a), we first see that just like in the case of spread Aloha, the header process is unable to follow the optimal $S = G$ curve as soon as the load increases beyond $G = 1$. However, in contrast to before, the difference between the header throughput and $S = G$ is less pronounced, even at a load of $G = 40$ transmissions. Essentially, the throughput in the (virtual) header channel diverges only slowly from optimal behavior. Hence, the remaining question to be answered is what fraction of this possible performance can be harnessed by the RP-CDMA data-detection stage. Proceeding from lowest to highest performance, we have the matched filter followed by decorrelation detection, collapsing at a load of $G = 18$ transmitters. This is easily exceeded with the MMSE, where the supportable number of transmissions equals $G = 27$ packets. Even higher performance can be achieved with partitioned spreading demodulation, where the maximum load approaches $G = 34$, in unison with [38, 39, 48]. For all the receivers, the throughput curves break down rapidly, indicating that after a certain load, the effective SINR after the detector was not sufficient for detection. As we focus our attention on the behavior of the queues in Figure 8(b), since the throughput in the virtual header channel diverges from $S = G$ instantly due to the limitations of the header process, the queues grow in size at all loads.

Fortunately, especially in packet-switched systems, P is very unrealistic, and of course, stable operation is very possible by adhering to the elements in $\mathbf{\Lambda}$.

6.1. Effect of the Header Frame on the Stability Region of RP-CDMA. Figure 9 summarizes our observations. There, we analyze the stable rates in the header and data channels separately and compare them to spread Aloha. Here, we see that in all cases of RP-CDMA data detection, the rate region formed by $\mathbf{\Lambda}^{(\text{eff})} = \min\{\mathbf{\Lambda}^{(h)}, \mathbf{\Lambda}^{(d)}\}$ is determined by the RP-CDMA header process. Interestingly, while especially from previous throughput plots, it seemed that upgrading the RP-CDMA data detection stage from matched filtering to partitioned spreading is necessary to increase the user base, in fact, as a result of the low supportable stable arrival rates in the virtual header channel, the rates for *all* of the additional users are diminishing to zero quickly. This leads to the following conclusion: due to the low stable header rates, the number of packets n' simultaneously "seen" by the receiver for the data stage is reduced. Hence, according to the definition of the conditional probabilities for reception, $\epsilon_{n,k} = p(k \text{ packets are correctly received} \mid n \text{ are active})$, depending on the actual performance in the header channel, simple linear multiuser receivers may be sufficient in the data stage even for large networks. As an example, at the point labeled as (20,0.25), $n = 20$ users can be active with a maximum arrival rate of $\lambda = 0.25$. From Figures 8 and 9, it seems that for such a network, at least a decorrelation receiver is required. However, with an expected number of simultaneous packets n' of $E[n'] = 20 \times 0.25 = 5$ in the virtual data channel, we see that, in fact, with a probability of $\epsilon_{5,5} = \mathbf{\Lambda}_5^{(\text{mf})} = 1$, the matched filter receiver is able to recover all transmissions. So while initially, a load of $n = 20$ indicated that matched filtering is not a sufficient choice for data detection of 20 users, due to the effects of the header channel which require low rates to maintain network stability, it may be all needed. Note, however, that the specific instantaneous traffic patterns (i.e., burstiness) may still require more advanced data detection.

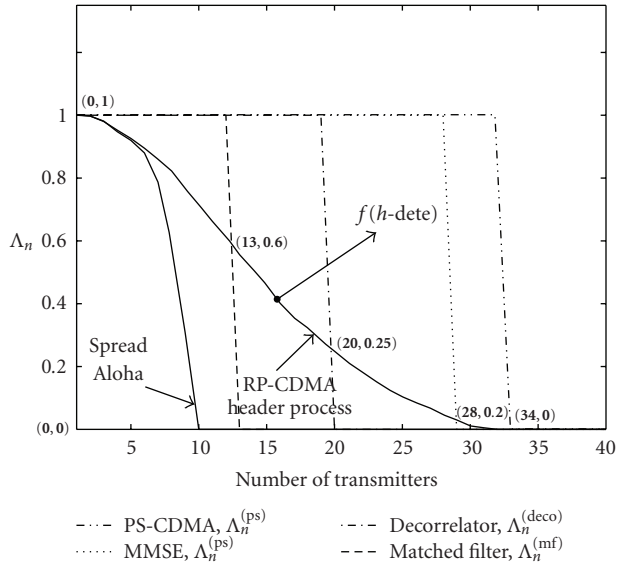

Figure 9: Comparison of user arrival rate regions which lead to network stability. $N_{\text{SA}} = N_d = N_h = 20$, trimodal packets and $L_h = 50$ bits such that $E[L_d/L_h] = 60$. $P_h/\sigma^2 = 15$ dB, $P_d/\sigma^2 = P_{\text{SA}}/\sigma^2 = 12$ dB. Detection thresholds of $\gamma_d = \gamma_{\text{SA}} = 3$ dB, $\gamma_h = 1$ dB. For partitioned spreading, $M = N_d/2 = 10$. As indicated by the arrow labeled $f(h - \text{dete})$, the area under the RP-CDMA header process generally increases as a function of $N_h, L_d/L_h, P_h/P_d$ and as $\gamma_h \to 0$.

Nevertheless, although it seems that there may be limited benefit in upgrading to partitioned spreading demodulation in certain cases, this may only be a part of the picture. It was shown in [38, 39, 48] that in contrast to other receiver methodologies, partitioned spreading allows to resolve virtually all multiuser interference. In our model, the rate regions for the various demodulators are formed by the packets whose SINR after the demodulator satisfy $\Gamma_i > \gamma$; this means that *we do not capture the degree* to which the SINRs exceed the detection threshold. Essentially, while the stable

arrival rates are determined by the header process, the usable *data rates* are determined by the demodulation scheme. As a result, even in our example with only 5 concurrent users in the data channel, partitioned spreading allows for *higher data rates* and, therefore, higher spectral efficiency. Another perspective on this issue is that for a targeted data rate, partitioned spreading demodulation allows to transmit the data frame at a lower SINR, therefore, making it possible to increase P_h/P_d which improves the performance in the header channel. As we have seen in Section 4, the behavior of the header process is nonlinear in some parameters and improving its performance directly faces limitations. Along these lines, upgrading RP-CDMA to partitioned spreading demodulation might be the easier and more practical way to improve performance.

Once more, we want to point that these observations are different from a conclusion one might draw based solely on the throughput curves in Figure 8, which may lead one to believe that matched filtering is *never* a satisfying candidate for the data demodulator as the network increases. Lastly, we recall that the area under the header-process generally increases with N_h, L_d/L_h, P_h/P_d and as $\gamma_h \to 0$, thus allowing to harness more of the performance of a more advanced data detection stage.

6.2. A Note on the Achievable Spectral Efficiency of RP-CDMA. Also as a result of our investigations, it is clear that the overall spectral efficiency $C^{(\text{eff})}$ of an RP-CDMA system is critically determined by its header process. Of course, trivially, the impact of the additional header frame on RP-CDMA system performance as well as on $C^{(\text{eff})}$ goes to zero as

$$N_h, \frac{L_d}{L_h}, \frac{P_h}{P_d} \longrightarrow \infty, \tag{43}$$

and/or the threshold for header detection γ_h:

$$\gamma_h \longrightarrow 0 \quad (\equiv -\infty \text{ dB}). \tag{44}$$

As the effect of the header diminishes, the performance of RP-CDMA is directly and only determined by the data-detection scheme. We want to refer the curious reader to [48] for a discussion on the achievable spectral efficiency of partitioned spreading.

7. Conclusions

We revisited RP-CDMA, a transmission scheme that was designed from the start as a cross-layer method and discussed its performance from a throughput and stability perspective. In contrast to previous works, our investigations were based on a realistic model for header and payload transmission. We showed how the characteristics of multipacket header reception on the physical layer make it possible to simplify the MAC layer, and at the same time allow to maintain very high system performance. While earlier results suggested that RP-CDMA throughput is only limited by the capabilities of the base station receiver as the ratio of data frame to header frame increases, we showed that, with a realistic model which takes multiuser interference into account, there is a point after which the RP-CDMA header process becomes *interference limited* instead of *header collision limited*, and increasing the ratio does not noticeably improve performance.

For the analysis of the quality of RP-CDMA payload detection, we compared the performance of partitioned spreading demodulation to the matched filter receiver, the decorrelator, and the MMSE filter. As expected, partitioned spreading greatly outperforms other reception methodologies, lead by the MMSE, the decorrelator, and finally the matched filter receiver.

We used two performance measures based on the modified multipacket capture matrix ($\widetilde{\mathbf{E}}$) termed ζ and $\mathbf{\Lambda}$. Through simulation, we showed that in equal power systems and with a transmission probability of $P = 1$, Λ_n presents an upper bound on the arrival rates $\boldsymbol{\lambda}$ which lead to network stability for n homogeneous (i.e., equal arrival rate, equal power) users. Also, since ζ is formed by summing the elements of $\mathbf{\Lambda}$, it can thus be used to capture the degree to which an accessing system or receiver is able to provide for user separation. Our analysis is supported by the theoretical works of Naware, Mergen and Tong in [5, 7, 8].

We simulated the throughput and delay characteristics of an RP-CDMA network and compared it to spread Aloha in a base station centric environment. Since the achievable stable arrival rates with RP-CDMA are critically determined by the header process and for additional users are diminishing to zero quickly, even for large networks, "weaker" multiuser receivers can be sufficient for the data stage. However, because of the vastly superior interference resolution capabilities and the near-far resistance of partitioned spreading, in all cases, much higher data rates can be used with such a demodulator—thus improving system performance.

Appendix

Let $u_i \geq 0$ denote the number of starting chips of packets in the ith chip, and note that when there are n active users,

$$u_1 + u_2 + u_3 + \cdots + u_N = n. \tag{A.1}$$

This equation has a total of $A_{\text{tot}}^{(A)} = \binom{n+N-1}{n}$ solutions. In a first step, we distribute the start of new packets in the N chips such that all k packets (and thus k transmissions) are successful. This is the case if the k packets are distributed over the total of N available chips, and $u_i \in (0, 1)$. In the next step, we distribute the remaining $(n - k)$, remembering that this time, the transmission is not successful, respectively. Since the k packets are successful, we can write the another equation as

$$u_1 + u_2 + u_3 + \cdots + u_{N-k} = n - k. \tag{A.2}$$

Furthermore, let m denote the u_i which have a value of $u_i = 0$, of which we have exactly $\binom{N-k}{m}$. In the rest of the chips, there are more than two starting chips of packets; therefore, we can write the new equation as

$$u_1 + u_2 + \cdots + u_{N-k-m} = n - k - 2(N - k - m), \quad u_i \geq 0, \tag{A.3}$$

which has a total number of solutions:

$$A_m^{(\mathrm{SA,coll})} = \binom{N-k-m-1+n-k-2(N-k-m)}{n-k-2(N-k-m)} = \binom{-N+m+n-1}{n+k-2N+2m}. \tag{A.4}$$

From here, the number of possible k survivals ($A_k^{(\mathrm{SA,coll})}$) out of n can be calculated as

$$A_k^{(\mathrm{SA,coll})} = \binom{N}{k} \sum_{\max(0,m_{\min})}^{N-k-1} \binom{N-k}{m} A_m^{(\mathrm{SA,coll})}, \tag{A.5}$$

where $m_{\min} \geq N-k-\lfloor (n-k)/2 \rfloor$, and

$$\epsilon_{n,k}^{(\mathrm{SA,coll})} = \frac{A_k^{(\mathrm{SA,coll})}}{A_{\mathrm{tot}}^{(\mathrm{SA,coll})}} = \frac{\binom{N}{k} \sum_{\max(0,m_{\min})}^{N-k-1} \binom{N-k}{m} A_m^{(\mathrm{SA})}}{\binom{n+N-1}{n}}. \tag{A.6}$$

Acknowledgments

The authors would like to thank Professor Christian Schlegel and Pooyan Amini for invaluable discussions related to partitioned spreading demodulation and combinatorics.

References

[1] T. S. Rappaport, *Wireless Communications: Principles and Practice*, Prentice-Hall, Upper Saddle River, NJ, USA, 2nd edition, 1996.

[2] W. Stallings, *Wireless Communications and Networks*, Prentice-Hall, Upper Saddle River, NJ, USA, 2nd edition, 2005.

[3] N. Abramson, "The ALOHA system—another alternative for computer communications," in *Proceedings of the Fall Joint Computer Conference (AFIPS '70)*, pp. 281–285, Houston, Tex, USA, November 1970.

[4] N. Abramson, "VSAT data networks," *Proceedings of the IEEE*, vol. 78, no. 7, pp. 1267–1274, 1990.

[5] V. Naware, G. Mergen, and L. Tong, "Stability and delay of finite-user slotted ALOHA with multipacket reception," *IEEE Transactions on Information Theory*, vol. 51, no. 7, pp. 2636–2656, 2005.

[6] C. Schlegel, R. Kempter, and P. Kota, "A novel random wireless packet multiple access method using CDMA," *IEEE Transactions on Wireless Communications*, vol. 5, no. 6, pp. 1362–1370, 2006.

[7] G. Mergen and L. Tong, "Stability and capacity of wireless networks with probabilistic receptions," Tech. Rep. ACSP-TR-01-03-01, Cornell University, Ithaca, NY, USA, 2003.

[8] Q. Zhao and L. Tong, "Semi-blind collision resolution in random access wireless ad hoc networks," *IEEE Transactions on Signal Processing*, vol. 48, no. 10, pp. 2910–2920, 2000.

[9] S. Verdú, *Multiuser Detection*, Cambridge University Press, Cambridge, UK, 1998.

[10] S. Verdú and S. Shamai, "Spectral efficiency of CDMA with random spreading," *IEEE Transactions on Information Theory*, vol. 45, no. 2, pp. 622–640, 1999.

[11] R. Lupas and S. Verdú, "Linear multiuser detectors for synchronous code-division multiple-access channels," *IEEE Transactions on Information Theory*, vol. 35, no. 1, pp. 123–136, 1992.

[12] A. J. Grant and P. D. Alexander, "Randomly selected spreading sequences for coded CDMA," in *Proceedings of the 4th IEEE International Symposium on Spread Spectrum Techniques Applications (ISSSTA '96)*, vol. 1, pp. 54–57, Mainz, Germany, September 1996.

[13] A. Goldsmith, *Wireless Communications*, Cambridge University Press, Cambridge, UK, 2006.

[14] C. Schlegel and L. Perez, *Trellis and Turbo Coding*, Wiley-IEEE Press, New York, NY, USA, 2004.

[15] D. I. Kim and J. C. Roh, "Performance of slotted asynchronous CDMA using controlled time of arrival," *IEEE Transactions on Communications*, vol. 47, no. 3, pp. 454–463, 1999.

[16] G. Mergen and L. Tong, "Stability and capacity of regular wireless networks," *IEEE Transactions on Information Theory*, vol. 51, no. 6, pp. 1938–1953, 2005.

[17] W. Luo and A. Ephremides, "Stability of N interacting queues in random-access systems," *IEEE Transactions on Information Theory*, vol. 45, no. 5, pp. 1579–1587, 1999.

[18] J. Luo and A. Ephremides, "Power levels and packet lengths in random multiple access with multiple-packet reception capability," *IEEE Transactions on Information Theory*, vol. 52, no. 2, pp. 414–420, 2006.

[19] J. Luo and A. Ephremides, "On the throughput, capacity, and stability regions of random multiple access," *IEEE Transactions on Information Theory*, vol. 52, no. 6, pp. 2593–2607, 2006.

[20] R. R. Rao and A. Ephremides, "On the stability of interacting queues in a multiple-access system," *IEEE Transactions on Information Theory*, vol. 34, no. 5, part 1, pp. 918–930, 1988.

[21] A. Ephremides and R.-Z. Zhu, "Delay analysis of interacting queues with an approximate model," *IEEE Transactions on Communications*, vol. 35, no. 2, pp. 194–201, 1987.

[22] S. Ghez, S. Verdú, and S. C. Schwartz, "Stability properties of slotted ALOHA with multipacket reception capability," *IEEE Transactions on Automatic Control*, vol. 33, no. 7, pp. 640–649, 1988.

[23] N. Abramson, "Fundamentals of packet multiple access for satellite networks," *IEEE Journal on Selected Areas in Communications*, vol. 10, no. 2, pp. 309–316, 1992.

[24] N. Abramson, "Multiple access in wireless digital networks," *Proceedings of the IEEE*, vol. 82, no. 9, pp. 1360–1370, 1994.

[25] D. R. Boggs, J. C. Mogul, and C. A. Kent, "Measured capacity of an Ethernet: myths and reality," in *Proceedings of the Symposium on Communications Architectures and Protocols (SIGCOMM '88)*, vol. 18, pp. 222–234, Stanford, Calif, USA, August 1988.

[26] R. M. Loynes, "The stability of a queue with non-independent inter-arrivals and service times," *Mathematical Proceedings of the Cambridge Philosophical Society*, vol. 58, no. 3, pp. 497–520, 1962.

[27] D. Raychaudhuri, "Stability, throughput, and delay of asynchronous selective reject ALOHA," *IEEE Transactions on Communications*, vol. 35, no. 7, pp. 767–772, 1987.

[28] V. Anantharam, "The stability region of the finite-user slotted ALOHA protocol," *IEEE Transactions on Information Theory*, vol. 37, no. 3, pp. 535–540, 1991.

[29] J. Wang and S. Keshav, "Efficient and accurate Ethernet simulation," in *Proceedings of the 24th Conference on Local Computer Networks (LCN '99)*, pp. 182–191, Lowell, Mass, USA, October 1999.

[30] M. C. Chan and R. Ramjee, "TCP/IP performance over 3G wireless links with rate and delay variation," in *Proceedings of the 8th Annual International Conference on Mobile Computing and Networking (MOBICOM '02)*, pp. 71–82, Atlanta, Ga, USA, September 2002.

[31] R. Kempter, *Modeling and evaluation of throughput, stability and coverage of RP-CDMA in wireless networks*, Ph.D. thesis, University of Utah, Salt Lake City, Utah, USA, December 2006.

[32] A. Yener and R. D. Yates, "Multiuser access detection for CDMA systems," in *Proceedings of the 32nd Annual Conference on Information Sciences and Systems (CISS '98)*, pp. 17–22, Princeton, NJ, USA, March 1998.

[33] A. Yener and R. D. Yates, "Multiuser access capacity of packet switched CDMA systems," in *Proceedings of the 49th IEEE Vehicular Technology Conference (VTC '99)*, vol. 3, pp. 1846–1850, Houston, Tex, USA, May 1999.

[34] A. Yener and R. D. Yates, "Acquisition dependent random access for connectionless CDMA systems," in *Proceedings of the IEEE Wireless Communications and Networking Conference (WCNC '00)*, vol. 1, pp. 173–178, Chicago, Ill, USA, September 2000.

[35] D. N. C. Tse and S. V. Hanly, "Linear multiuser receivers: effective interference, effective bandwidth and user capacity," *IEEE Transactions on Information Theory*, vol. 45, no. 2, pp. 641–657, 1999.

[36] R. Kempter, P. Amini, C. Schlegel, and B. Farhang-Boroujeny, "On coverage and routing in wireless ad hoc networks," *IEEE Signal Processing Magazine*, vol. 23, no. 5, pp. 50–62, 2006.

[37] Z. Bagley and C. Schlegel, "Implementation of digital timing recovery," L-3 Communications patent application filed with Perman and Green, LLP, Fairfield, Conn, USA, 2001.

[38] C. Schlegel, "CDMA with partitioned spreading," *IEEE Communications Letters*, vol. 11, no. 12, pp. 913–915, 2007.

[39] R. Kempter and C. Schlegel, "Packet random access in CDMA radio networks," in *Proceedings of the 43rd Annual Allerton Conference on Communication, Control and Computing*, pp. 986–995, Monticello, Ill, USA, September 2005.

[40] C. Berrou and A. Glavieux, "Near optimum error correcting coding and decoding: turbo-codes," *IEEE Transactions on Communications*, vol. 44, no. 9, pp. 1261–1271, 1996.

[41] A. J. Viterbi, *CDMA: Principles of Spread Spectrum Communications*, Addison-Wesley, Menlo Park, Calif, USA, 1995.

[42] C. Schlegel and A. Grant, *Coordinated Multiple User Communications*, Springer, New York, NY, USA, 2005.

[43] M. V. Burnashev, C. B. Schlegel, W. A. Krzymien, and Z. Shi, "Analysis of the dynamics of iterative interference cancellation in iterative decoding," *Problems of Information Transmission*, vol. 40, no. 4, pp. 297–317, 2004.

[44] "Statistics for the Abilene backbone network of Internet2," 2005, http://netflow.internet2.edu/.

[45] C. Schlegel and R. Kempter, "Random-packet CDMA: a novel wireless packet system," in *iCORE Summit Plenary Presentation*, Banff, Canada, June 2004.

[46] R. Kempter and C. Schlegel, "Capacity and QoS analysis for a novel packet based wireless access system," in *Proceedings of the 58th IEEE Vehicular Technology Conference (VTC '03)*, vol. 3, pp. 1432–1436, Orlando, Fla, USA, October 2003.

[47] R. Tandra, *Fundamental limits on detection in low SNR*, M.S. thesis, University of California, Berkeley, Calif, USA, May 2005.

[48] Z. Shi, C. Schlegel, R. Kempter, and M. C. Reed, "On the performance of partitioned-spreading CDMA with multistage demodulation," in *Proceedings of the 40th Annual Conference on Information Sciences and Systems (CISS '07)*, pp. 1522–1527, Princeton, NJ, USA, March 2007.